

From Charts to Atlas: Merging Latent Spaces into One

Donato Crisostomi

Sapienza University of Rome

CRISOSTOMI@DI.UNIROMA1.IT

Irene Cannistraci

Sapienza University of Rome

CANNISTRACI@DI.UNIROMA1.IT

Luca Moschella

Sapienza University of Rome

MOSCHELLA@DI.UNIROMA1.IT

Pietro Barbiero

University of Cambridge

PB737@CAM.AC.UK

Marco Ciccone

Politecnico di Torino

MARCO.CICCONE@POLITO.IT

Pietro Liò

University of Cambridge

PL219@CAM.AC.UK

Emanuele Rodolà

Sapienza University of Rome

RODOLA@DI.UNIROMA1.IT

Editors: Sophia Sanborn, Christian Shewmake, Simone Azeglio, Nina Miolane

Abstract

Models trained on semantically related datasets and tasks exhibit comparable inter-sample relations within their latent spaces. We investigate in this study the aggregation of such latent spaces to create a unified space encompassing the combined information. To this end, we introduce Relative Latent Space Aggregation (RLSA), a two-step approach that first renders the spaces comparable using relative representations, and then aggregates them via a simple mean. We carefully divide a classification problem into a series of learning tasks under three different settings: sharing samples, classes, or neither. We then train a model on each task and aggregate the resulting latent spaces. We compare the aggregated space with that derived from an end-to-end model trained over all tasks and show that the two spaces are similar. We then observe that the aggregated space is better suited for classification, and empirically demonstrate that it is due to the unique imprints left by task-specific embedders within the representations. We finally test our framework in scenarios where no shared region exists and show that it can still be used to merge the spaces, albeit with diminished benefits over naive merging.

1. Introduction

The success of neural networks can partly be attributed to the latent spaces they learn. In fact, given a sufficiently general task, the deeper layers of a network are able to learn semantically meaningful representations that capture the inherent data structure. If these representations solely relied on semantics, the latent space would exhibit invariance to the model's architecture and training process and be seamlessly transferable to other tasks sharing the same semantics. In practice, however, training stochasticities such as initialization and data shuffling hinder the immediate comparability of latent spaces. Nevertheless, when spaces are rich in semantics, the distance between data points becomes indicative of their similarity.

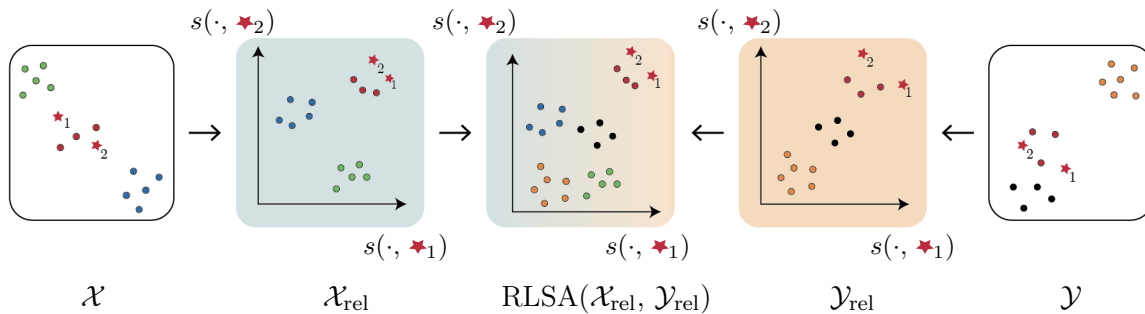


Figure 1: **Framework description.** Given two absolute spaces \mathcal{X} and \mathcal{Y} , we first project these spaces into two comparable relative representations \mathcal{X}_{rel} , \mathcal{Y}_{rel} . Then, we combine these representations into a single, unified relative space $\text{RLSA}(\mathcal{X}_{\text{rel}}, \mathcal{Y}_{\text{rel}})$.

That is, samples located close to each other are likely to share similarities, and conversely, those farther apart are expected to be more distinct. This intuitive notion suggests that the latent spaces of models trained on semantically analogous datasets and tasks relying on the same underlying structure should exhibit similar inter-sample relations. Returning to a geometric perspective, this implies that the inter-sample distances should remain consistent across the two spaces. Building upon this insight, Moschella et al. (2023) introduced relative representations as a way to compare latent spaces: when the similarities among samples are consistent across the two spaces, the latter become comparable.

In this paper, we investigate a natural follow-up question: when, and under what assumptions, *can two spaces be merged into one?* In principle, given two comparable representations that may partially overlap or be entirely disjoint, it should be possible to generate a unified representation in which both coexist consistently. We refer to this problem as *Latent Space Aggregation*. Space aggregation raises several questions on i) the representational power of the unified representation space, ii) its ability to accommodate both spaces without collisions, and iii) its robustness to complementary information present in only one of the two spaces. In fact, naively aggregating the sample representations by computing their mean *in absolute coordinates* would not account for the different latent configurations caused by training stochasticities, resulting in an inconsistent aggregation of different entities based on spurious random factors.

Motivated by the above challenges, we propose Relative Latent Space Aggregation (RLSA). Our approach involves two steps: we first switch to a relative representation where the latent spaces are represented with respect to a set of anchors, and then aggregate the obtained representations by computing their mean. The first step makes the spaces comparable, enabling a meaningful aggregation of samples that are common to multiple latent spaces, at the same time avoiding collisions.

To test our framework, we partition a classification dataset into multiple learning *tasks*. These tasks can vary in terms of class composition, such as covering disjoint subsets of classes, or in sample composition, such as being sampled with different class distributions. These diverse tasks enable us to train task-specific models, extract their latent spaces, and subsequently examine their aggregation. We consider three different cases: i) tasks sharing a set of samples, ii) tasks sharing the same classes but disjoint sample sets, and iii) tasks

disjoint both at the class and at the sample level. In the first case, we select the anchors from the shared samples, while in the disjoint scenarios they are sampled from unseen samples in the training dataset. We then analyze the quality of the aggregation by i) comparing it to the space of an end-to-end model trained on all the tasks, ii) assessing the performance of a classifier over the aggregated space, and iii) quantifying the separability of the classes within it. We show that the best results are obtained when sharing samples, while the benefits decrease in the disjoint scenarios. Finally, we release an extensible and modular codebase¹ to foster reproducibility and further research in the problem.

To summarize, our contributions are three-fold:

1. We propose for the first time a framework for latent space aggregation, merging different latent spaces without requiring weight averaging, sharing, or any model-specific details;
2. We evaluate our framework on aggregating tasks sharing samples, classes, or neither, assessing representational power, class separability, and similarity to the global space;
3. We investigate the improved performance over class-disjoint tasks, empirically demonstrating that it is a natural consequence of utilizing task-specific embedders.

2. Related work

Closest to our work are the fields of model merging and representational similarity analysis. In model merging, the goal is to combine multiple models into a single model. This is usually done by merging the models’ parameters with some aggregation function, *e.g.*, by averaging (McMahan et al., 2017). Most recently, Git Re-Basin (Ainsworth et al., 2022) leverages advances in linear mode connectivity (Garipov et al., 2018; Benton et al., 2021; Frankle et al., 2019) to first map the two models into the same basin, and then interpolate among them. It is important to note that, unlike model merging, *our approach does not require any architectural details from the models* and is therefore applicable to a set of spaces originating from any set of models. On the other hand, our approach does not provide a trained model, but rather a unified space that can be used as a starting point to train other models.

In representational similarity analysis, the goal is to compare the representations of different models. Several measures have been proposed for the task (Klabunde et al., 2023; Shahbazi et al., 2021; Raghu et al., 2017; Tang et al., 2020; Williams et al., 2021), with the most prominent being Centered Kernel Alignment (CKA) (Kornblith et al., 2019). In this work, we use CKA to compare the representations of the models in the aggregated space.

3. Approach

Relative representations We leverage relative representations (Moschella et al., 2023) to render the seemingly different latent spaces comparable. In practice, we start by selecting a subset \mathbb{A} of the training data \mathcal{X} , denoted as anchor samples. Every sample in the training distribution will be represented as a function of the embedded anchors $\mathbf{a}_j = f_{\Theta}(a_j)$ with $a_j \in \mathbb{A}$. As a measure capturing the relation between the anchors and the other samples, we consider the cosine similarity $s : \mathbb{R}^d \times \mathbb{R}^d \mapsto \mathbb{R}$, yielding a scalar score $r \in [-1, 1]$ between

1. <https://github.com/crisostomi/latent-aggregation>

two absolute representations $\mathbf{x}_i, \mathbf{x}_j$. The relative representation of $x_i \in \mathcal{X}$ as a function of the anchors \mathbb{A} is then given by

$$r(x_i) = (s(\mathbf{x}_i, \mathbf{a}_1), s(\mathbf{x}_i, \mathbf{a}_2), \dots, s(\mathbf{x}_i, \mathbf{a}_{\|\mathbb{A}\|})) \quad (1)$$

In the following, we will call the embedding space the *absolute space*, and the set of relative representations the *relative space*.

Space aggregation Given a set of M relative spaces $X_r^{(1)}, \dots, X_r^{(M)}$, we can define an aggregation function that maps them to a single space. If a sample x appears in $K \leq M$ spaces, we can assemble its relative representations $x_r^{(1)}, \dots, x_r^{(K)}$ just by taking their mean:

$$x_{\text{aggregated}} = \frac{1}{K} \sum_{k=1}^K X_r^{(k)}. \quad (2)$$

This trivially entails that when the spaces are disjoint, each sample representation will just be its relative representation in its original space. The aggregation accounts for noise in the relative representations, as the same samples may be represented differently in the different relative spaces. Nevertheless, in the optimal case in which they perfectly align, the relative representation will be equal for all the spaces and therefore still equal to the mean. Due to the different experimental settings, the anchor set is chosen differently for each scenario. In particular, when a portion of samples is shared, we select our anchors there. In fact, these are samples that the model can reliably embed in the latent space and can be used as reference points to give structure to the new aggregated space. Intuitively, if the resulting latent regions are comparable and shared, the out-of-distribution samples should be triangulated in a consistent manner. On the other hand, when the tasks are disjoint, the anchors are extracted from a small subset of the global dataset that is not shown to the model. Indeed, if these were used for training, the task-specific models would be partially aware of the overall class distribution, while we enforce them to see only the samples and classes of the task they are trained on. Importantly, the projection anchors are the same across all the tasks. Within the anchor set, we follow [Moschella et al. \(2023\)](#) and employ random sampling.

4. Experiments

We consider two datasets throughout our experiments: CIFAR100 ([Krizhevsky et al., 2009](#)) and TinyImagenet ([Le and Yang, 2015](#)). We refer to the latter as TINY in the tables for brevity. These offer a good trade-off between scale and tractability. In fact, the first experiment alone requires training and aggregating 70 task-specific models. Dataset details can be found in appendix [A.1](#). As for the models, we experiment with a standard convolutional neural network trained from scratch and a pre-trained EfficientNet due to its superior performance on CIFAR100 ([Tan and Le, 2019](#)). Common to the experiments will be a quantitative measure of the similarity between the aggregated space and the space of a model trained end-to-end on the whole dataset. To this end, we employ CKA ([Kornblith et al., 2019](#)) as it is the most commonly used metric for comparing neural representations. We measure the separability of the considered spaces as the ratio of the inter-class distances over the average of the intra-class distances. The latter is described in detail in appendix [C.3](#). For space reasons, we will consider only one of the datasets or a subset of the configurations when the results are consistent, reporting the remaining experiments in appendix [B.3](#).

Dataset	S	N	# tasks	CKA					
				non-shared	shared	overall	non-shared	shared	overall
CIFAR100				VanillaCNN			EfficientNet		
	80	10	2	0.88	0.90	0.90	0.85	0.90	0.89
	60	10	4	0.85	0.92	0.89	0.82	0.88	0.85
	40	10	6	0.83	0.91	0.86	0.80	0.89	0.83
	20	10	8	0.74	0.86	0.76	0.77	0.87	0.79
	80	5	4	0.90	0.93	0.92	0.81	0.90	0.88
	60	5	8	0.82	0.90	0.87	0.83	0.87	0.84
	40	5	12	0.81	0.87	0.84	0.78	0.89	0.82
20	5	16	0.78	0.87	0.80	0.77	0.88	0.79	
TINY				VanillaCNN			EfficientNet		
	100	25	4	0.85	0.91	0.88	0.72	0.81	0.76
	50	25	6	0.83	0.91	0.85	0.67	0.80	0.71

Table 1: **Experiment 1.** Comparison of the aggregated spaces with the space of an end-to-end model trained on the whole dataset. S and N represent the number of shared and novel classes per task out of a total of C classes. We compute CKA both for the *overall* space and for the subspaces defined by *non-shared* and *shared* classes.

Dataset	S	N	tasks	vanilla	non-shared	shared	total	improv	vanilla	non-shared	shared	total	improv
CIFAR100				VanillaCNN				0.39	EfficientNet				0.70
	80	10	2	0.36	0.60	0.39	0.43	+0.04	0.68	0.80	0.71	0.73	+0.02
	60	10	4	0.39	0.64	0.45	0.53	+0.14	0.72	0.82	0.76	0.79	+0.08
	40	10	6	0.42	0.64	0.50	0.58	+0.19	0.75	0.87	0.80	0.84	+0.14
	20	10	8	0.47	0.65	0.52	0.62	+0.23	0.80	0.88	0.84	0.87	+0.17
	80	5	4	0.37	0.77	0.41	0.49	+0.10	0.71	0.84	0.72	0.75	+0.05
	60	5	8	0.39	0.71	0.45	0.55	+0.16	0.76	0.85	0.78	0.81	+0.11
	40	5	12	0.44	0.74	0.49	0.64	+0.25	0.80	0.90	0.80	0.86	+0.16
20	5	16	0.51	0.76	0.55	0.72	+0.33	0.83	0.93	0.83	0.90	+0.20	
TINY				VanillaCNN				0.22	EfficientNet				0.69
	100	25	4	0.22	0.37	0.23	0.30	+0.08	0.68	0.75	0.71	0.73	+0.05
	50	25	6	0.24	0.36	0.36	0.36	+0.14	0.72	0.77	0.74	0.77	+0.08

Table 2: Classification accuracy comparison. Each quarter shows a dataset-model combination, with end-to-end model accuracy on the right. For each S , N combination, we report the accuracy of a classifier trained on the aggregated space, along with accuracy when considering only *non-shared* and *shared* classes. *Improv* is the improvement over the end-to-end model, while *vanilla* the accuracy of naive merging.

that it is enough to merge the spaces without first passing to a unified representation, we also test with a classifier trained on the union of the absolute embedding spaces. As we can see in table 2, the performance is way lower than that of the classifier trained on the aggregated space, confirming that the relative representation is beneficial.

To check whether different non-shared classes end up in the same region in the aggregated space, we measure the mean separability for any pair of classes c_i, c_j such that either is not

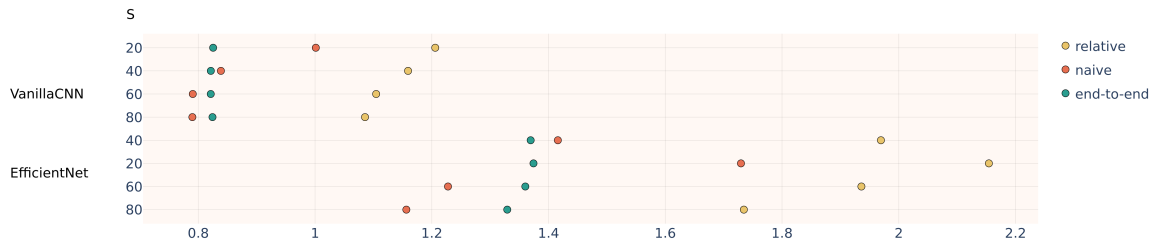


Figure 3: Separability analysis over CIFAR100: we compare the mean separability of the resulting space when using relative and naive aggregation for different values of S and $N = 10$, as well as the separability over the space of the end-to-end model trained over the whole dataset. The relatively aggregated space consistently results in the highest separability.

shared. Figure 3 shows that our approach is consistently higher than the baseline, suggesting that the former can better avoid collisions from the merge. Surprisingly, the separability of the aggregated space is also higher than that of the end-to-end one, and it is higher for smaller numbers of shared classes. This again suggests that the task-specific models can better separate the samples and that the aggregated space can preserve this information.

Summary Aggregating spaces of models trained on tasks sharing a portion of samples results in a space that is similar to the one of the end-to-end model but that allows significantly better classification performance and improved class separability, especially when task-specific models have fewer shared classes.

4.2. Aggregating tasks sharing classes

Setup In this experiment, we divide the dataset into two disjoint subsets, A and B . Subset A comprises 20% samples labeled from the first half of the classes and 80% instances labeled from the second one, while subset B contains 80% samples labeled from the first and 20% samples labeled from the second. This arrangement ensures a distributional imbalance in terms of class labels between the two subsets. Subsequently, we train two models on A and B ; each model learns to classify the distinct distribution of labels within its assigned subset. Post-training, we introduce an unseen set of anchor points to project the latent spaces of the two models to relative spaces.

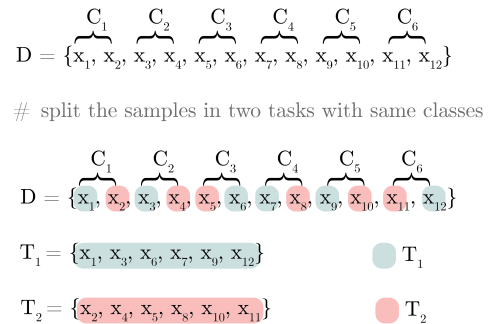


Figure 4: Experiment outline.

The final step involves unifying these relative spaces into a single latent space: similarly to the samples belonging to novel classes in Section 4.1, we only have one representation for each sample already in the unified latent space.

Results Figure 5 shows that, in this case, relative aggregation does not improve over naive merging when considering classification accuracy. This suggests that a shared region of the latent space is required for the relative representations to be most effective. However, fig. 12 shows that the relative aggregated space still vastly outperforms the naive one regarding class

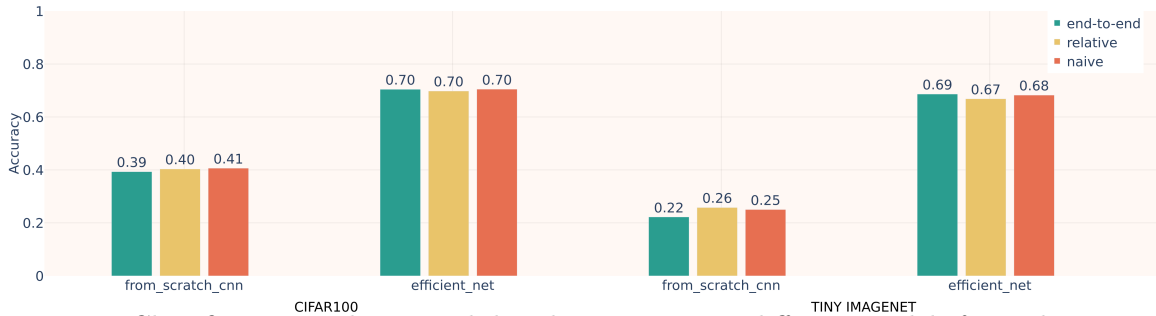


Figure 5: Classification analysis. Each barplot represents a different model: for each one; we compare its *end-to-end* accuracy versus that of a classifier trained over the *relative* aggregated space and that of a classifier trained over the *naive* aggregated space.

separability. This last result hints at the relative aggregated space being better suited for classification, attributing the equality in results with the naive baseline to the expressiveness of the downstream classifier that can make up for the inferior separability of the naive space.

It is noteworthy to observe that the aggregated spaces, both the naive and the relative ones, can reach a comparable accuracy to the end-to-end model. This is a remarkable result, as it shows that the unified space can capture the information from both models, even though the two models were trained on disjoint tasks. This is further confirmed by the similarity between original and relative aggregated being as high as 0.87, 0.83 on CIFAR100 for EfficientNet and VanillaCNN respectively, and 0.79 and 0.84 on TinyImagenet.

Summary For sample-disjoint tasks sharing common classes but distinct distributions, the relative aggregated space effectively preserves information from both spaces, improving classification accuracy and class separability in downstream tasks.

4.3. Aggregating totally disjoint tasks

Setup Similarly to section 4.2, we split a dataset into two disjoint sets of samples, with the difference that these now also belong to disjoint class sets. The first set comprises samples exclusively from the first half of the classes, while the second consists of samples from the remaining half. This ensures that the two subsets do not overlap in classes or instances, presenting an independent learning scenario for two models to be trained on. Post-training, we introduce an unseen set of anchor points spanning all the classes, and use them to project the latent spaces into relative spaces.

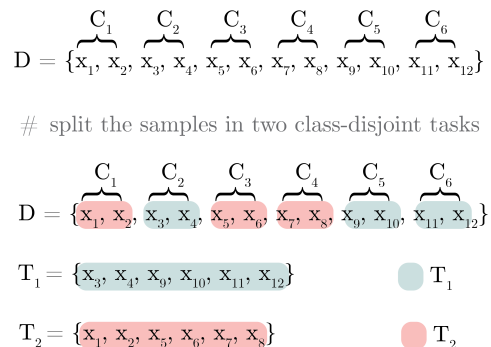


Figure 6: Experiment outline.

In this way, each task-specific space will be projected with respect to anchors that are roughly half from the training distribution and half from out-of-distribution. Coming from disjoint tasks, each sample will then just be represented with its relative representation.

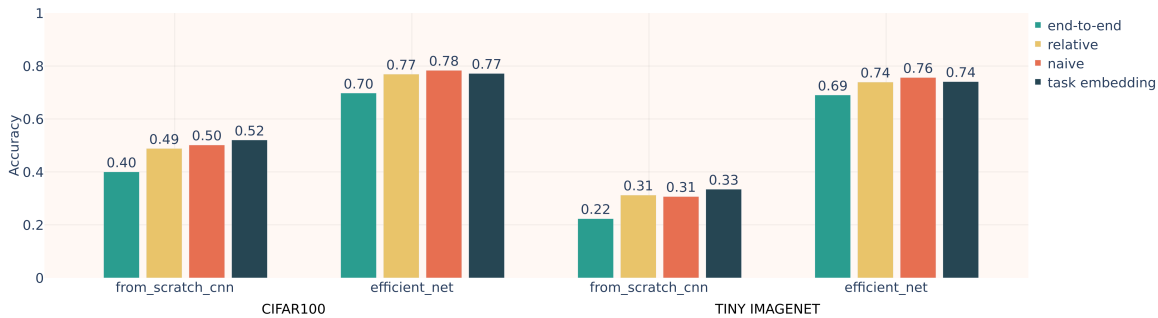


Figure 7: Classification analysis. Each barplot represents a different model: for each one; we compare its *end-to-end* accuracy versus that of a classifier trained over the *relative* aggregated space and that of a classifier trained over the *naive* aggregated space.

Results As the spaces to aggregate are class- and sample-disjoint, the similarity to the end-to-end space drops to 0.81, 0.83 on CIFAR100 and to 0.72, 0.81 on TinyImageNet for EfficientNet and VanillaCNN respectively. Interestingly, fig. 7 shows that the space that allows us to obtain the best results is consistently the aggregated one, significantly outperforming the original space obtained by training a model end-to-end over the whole dataset. While surprising, this finding aligns with the increased performance over the tasks with fewer shared classes seen in Section 4.1. We envision two possibilities to explain this phenomenon. **Hypothesis A:** The task-specific models can extract more specialized features for their classes, presenting the downstream classifier with better features. To investigate this hypothesis, we start from the first three classes $C_1 = c_1, c_2, c_3$ of CIFAR100 and gradually expand the set with a new class c_i for $i = 1, \dots, M$. We train a model on each class set $\{c_1, c_2, c_3\}, \dots, \{c_1, \dots, c_M\}$, use it to embed the samples with class in C_1 and then train a downstream classifier on this embedding space. Intuitively, the embeddings for three original classes will come from increasingly more crowded spaces with the addition of new classes. Figure 8 shows that the accuracy has an increasing trend overall when adding new classes, therefore not supporting the hypothesis. Similarly, the second experiment in appendix B.3 compares the classification suitability of the embeddings of M classes in a task-specific space versus the embeddings of the same classes in the space of all the C classes. As before, the restriction over the M classes in the space of a model trained on all C classes proves a better feature space than the space of a model that is only trained over the M classes, again disconfirming the hypothesis. **Hypothesis B:** the task-specific models trained on $C' \leq C$ classes leave a footprint in the embeddings, allowing the downstream classifier to discriminate among a smaller set of classes. To verify whether this holds, we add a task-embedding layer to the downstream classifier and train it on the embedding space of the end-to-end model. The results, shown in Figure 7, show that the accuracy rises to that of the aggregation techniques, confirming the hypothesis. Intuitively, being trained on a smaller subset of classes, the task-specific embedders are better able to discriminate their class set. If the embeddings carry a footprint of the model, they also covertly reveal the task. The downstream classifier can exploit this information and discriminate among C' classes instead of C , significantly lowering the complexity of the task and therefore increasing its accuracy.

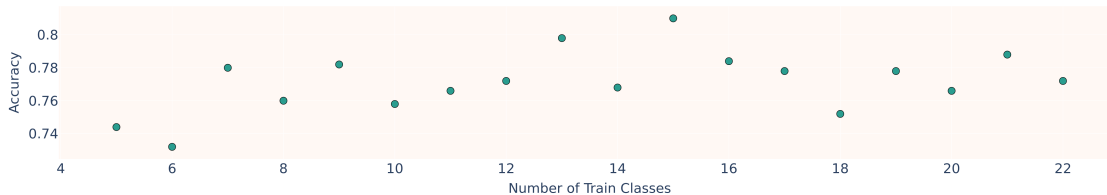


Figure 8: Classifier accuracy as the embedding space becomes less specific, where point i represents the accuracy of a downstream classifier over classes c_1, c_2, c_3 embedded within a space containing classes $c_1, c_2, c_3, \dots, c_{i+3}$.

Summary Relative aggregation allows merging sample- and class-disjoint spaces, granting better accuracy than an end-to-end model trained over the whole dataset due to task-specific footprints being embedded within the representations.

5. Conclusions

In this work, we have studied the problem of aggregating spaces originating from different learning models, possibly more than one. We have seen how relative representations provide the means to perform this operation and analyzed various experimental settings spanning a set of varying assumptions. In particular, we have seen that the approach works best when a shared region of the space is available, and that it is still possible to obtain good results when this is not the case. We have studied the characteristics of the aggregated space in terms of representational power, separability, and similarity to an end-to-end space trained over the whole dataset, and have shown the benefits of the approach when compared to a naive merging baseline. In future work, we envision applying the approach to other settings, such as federated learning, where aggregating latent spaces involving anonymized anchors could provide an architecture-agnostic alternative to weight-space model merging.

References

- Samuel K Ainsworth, Jonathan Hayase, and Siddhartha Srinivasa. Git Re-Basin: Merging models modulo permutation symmetries. September 2022.
- Gregory W Benton, Wesley J Maddox, Sanae Lotfi, and Andrew Gordon Wilson. Loss surface simplexes for mode connecting volumes and fast ensembling. February 2021.
- Jonathan Frankle, Gintare Karolina Dziugaite, Daniel M Roy, and Michael Carbin. Linear mode connectivity and the lottery ticket hypothesis. December 2019.
- Timur Garipov, Pavel Izmailov, Dmitrii Podoprikin, Dmitry Vetrov, and Andrew Gordon Wilson. Loss surfaces, mode connectivity, and fast ensembling of DNNs. February 2018.
- Max Klabunde, Tobias Schumacher, Markus Strohmaier, and Florian Lemmerich. Similarity of neural network models: A survey of functional and representational measures. *arXiv [cs.LG]*, May 2023.

- Simon Kornblith, Mohammad Norouzi, Honglak Lee, and Geoffrey Hinton. Similarity of neural network representations revisited. May 2019.
- Alex Krizhevsky et al. Learning multiple layers of features from tiny images. 2009.
- Ya Le and Xuan Yang. Tiny imagenet visual recognition challenge. *CS 231N*, 7(7):3, 2015.
- Brendan McMahan, Eider Moore, Daniel Ramage, Seth Hampson, and Blaise Aguera y Arcas. Communication-efficient learning of deep networks from decentralized data. In *Artificial intelligence and statistics*, pages 1273–1282. PMLR, 2017.
- Luca Moschella, Valentino Maiorca, Marco Fumero, Antonio Norelli, Francesco Locatello, and Emanuele Rodolà. Relative representations enable zero-shot latent space communication, 2023.
- Maithra Raghu, Justin Gilmer, Jason Yosinski, and Jascha Sohl-Dickstein. SVCCA: Singular vector canonical correlation analysis for deep learning dynamics and interpretability. June 2017.
- Mahdiyar Shahbazi, Ali Shirali, Hamid Aghajani, and Hamed Nili. Using distance on the riemannian manifold to compare representations in brain and in models. *Neuroimage*, 239: 118271, October 2021.
- Mingxing Tan and Quoc Le. Efficientnet: Rethinking model scaling for convolutional neural networks. In *International conference on machine learning*, pages 6105–6114. PMLR, 2019.
- Shuai Tang, Wesley J Maddox, Charlie Dickens, Tom Diethe, and Andreas Damianou. Similarity of neural networks with gradients. March 2020.
- Alex H Williams, Erin Kunz, Simon Kornblith, and Scott W Linderman. Generalized shape metrics on neural representations. October 2021.

Appendix A. Details

We report here the technical details that are not present in the main manuscript.

A.1. Dataset details

We employ two well-established benchmark datasets that offer a good trade-off between scale and tractability. In fact, the first experiment alone requires training and aggregating 70 task-specific models.

CIFAR100 CIFAR-100 (Krizhevsky et al., 2009) is a popular dataset in the field of computer vision. It consists of 100 different classes, each containing 600 images, making a total of 60,000 labeled images for training and testing. CIFAR-100 is widely used for benchmarking and evaluating the performance of machine learning and deep learning models in tasks such as image classification and object recognition. It offers a diverse range of objects and scenes, making it a challenging dataset for developing and testing algorithms in the field of image analysis and pattern recognition.

TinyImageNet TinyImageNet is a subset of the larger ImageNet dataset, focusing on a more manageable scale while maintaining its diversity. It consists of 100000 images of 200 classes (500 for each class) downsized to 64×64 colored images. Each class has 500 training images, 50 validation images and 50 test images.

A.2. Model details

All our models are trained using the Adam optimizer from the *torch.optim* suite.

VanillaCNN We utilized a vanilla Convolutional Neural Network (CNN). The model is defined by intermediate convolutional stages with 16 and 32 channels respectively, culminating in an embedding layer of 128 dimensions. The preprocessing pipeline only consists of normalization.

EfficientNet We employ EfficientNet as a pre-trained model for our experiments, specifically the *efficientnet_b0* variant provided by the *TIMM* library. Post the embedder, we employ a MultiLayer Perceptron (MLP) projector, which transitions from an input feature dimension of 1280 to a hidden dimension of 256, and ultimately to a projection dimension of 128. As for preprocessing, images are first converted to the PIL format, resized to 256 pixels on the longer side, and then center-cropped to a consistent size of 224×224 pixels. Standard normalization ensures the input images are aptly conditioned for the model’s requirements.

A.3. Tools & Technologies

We use the following tools in all the experiments presented in this work:

- *PyTorch Lightning*, to ensure reproducible results while also getting a clean and modular codebase;
- *NN-Template GrokAI (2021)*, to easily bootstrap the project and enforce best practices;
- *Datasets by HuggingFace*, to access the datasets.

Appendix B. Additional experiments

We report here the results for the experiment configurations that were omitted in the manuscript, as well as experiments that were only mentioned.

B.1. Qualitative visualization

Figure 9 compares the space of an end-to-end model trained on the whole dataset and the aggregated space from the task-specific models. Being the hardest to position, only the non-shared classes are visualized. Remarkably, even in this case, the aggregated spaces look similar to the one of the end-to-end model.

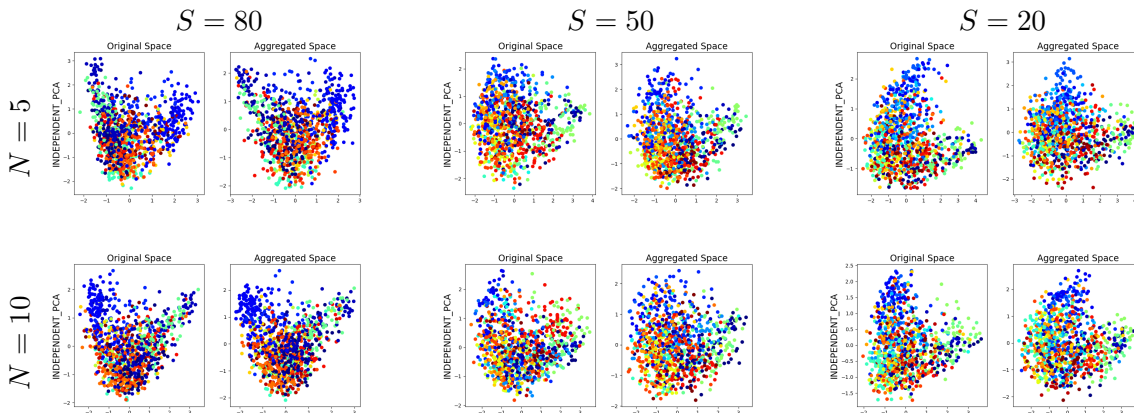


Figure 9: Experiment 1. Principal Component Analysis (PCA) visualizations of the latent space obtained training on the whole dataset versus aggregated latent spaces from models trained on partially disjoint tasks. Notably, the spaces remain similar despite reducing the shared core of classes.

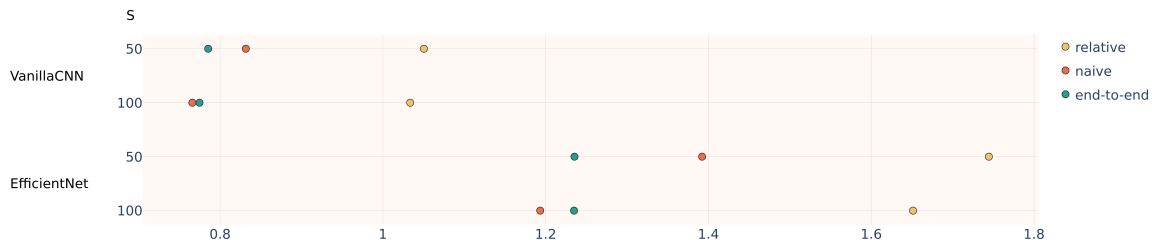


Figure 10: Separability analysis over TinyImageNet for tasks sharing a sample portion: we compare the mean separability of the resulting space when using relative and naive aggregation for different values of S and $N = 25$, as well as the separability over the space of the end-to-end model trained over the whole dataset. The relatively aggregated space consistently results in the highest separability.

B.2. Separability analysis

Figure 11 shows the separability for the spaces obtained in section 4.1 for $N = 5$. The same considerations given for $N = 10$ apply. Figure 10 instead shows the same analysis for TinyImageNet. In Figure 12, we instead show the separability values for the aggregation of sample-level disjoint tasks, as described in section 4.2. In Figure 13 the same analysis is carried for spaces that are disjoint at the class and sample level, as described in section 4.3.

B.3. Subclass experiment

In this experiment, we compare the classification suitability of the embeddings of M classes in a task-specific space versus the embeddings of the same classes in the space of all the C classes. In practice, we randomly sample M classes for each task, train a model on the corresponding sample subset, and then use it to embed an unseen test dataset for the same classes. We then also train a model from scratch over the whole dataset, and use it to

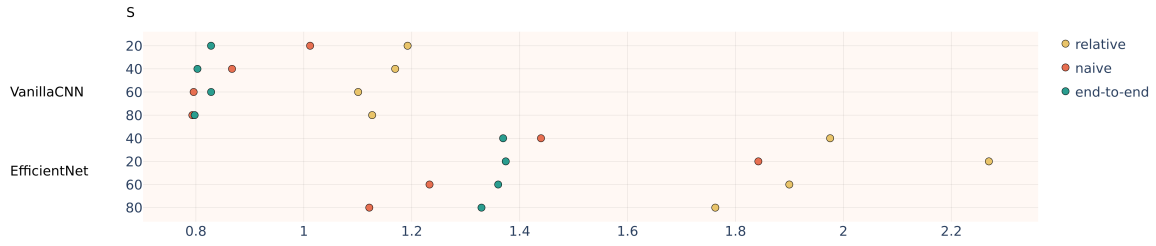


Figure 11: Separability analysis over CIFAR100 for tasks sharing a sample portion: we compare the mean separability of the resulting space when using relative and naive aggregation for different values of S and $N = 5$, as well as the separability over the space of the end-to-end model trained over the whole dataset. The relatively aggregated space consistently results in the highest separability.

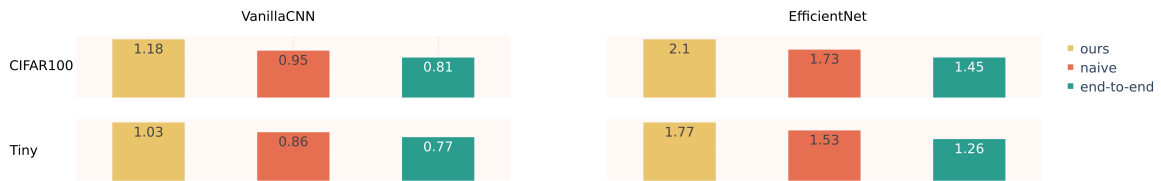


Figure 12: Separability analysis over CIFAR100 and TinyImageNet for sample-level disjoint tasks sharing the same class set: we plot the mean separability over the relatively aggregated space, the naively aggregated space, and the one of the end-to-end model. The relatively aggregated space consistently results in the highest separability.

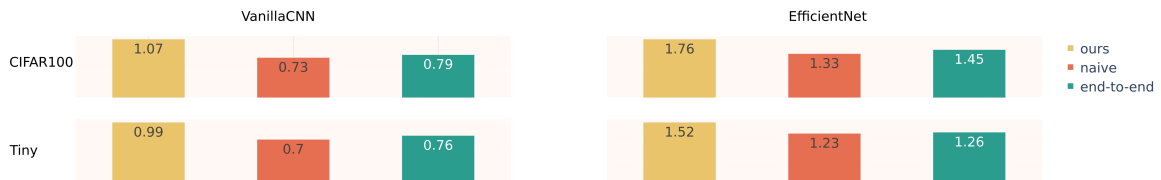


Figure 13: Separability analysis over CIFAR100 and TinyImageNet for tasks disjoint both at the sample and at the class level: we plot the mean separability over the relatively aggregated space, the naively aggregated space, and the one of the end-to-end model. The relatively aggregated space consistently results in the highest separability.

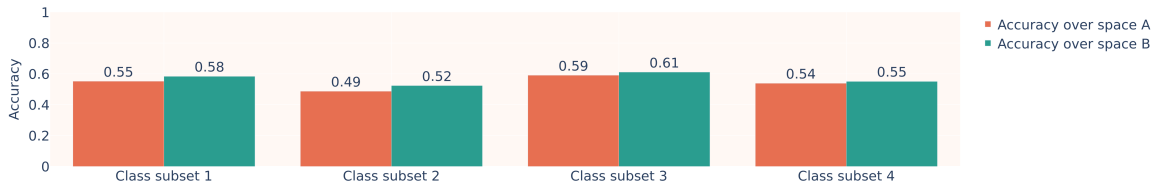


Figure 14: Accuracy results for the experiment in appendix B.3. Each barplot is a different task, space A is the feature space learned by the model trained on $M = 30$ classes, and space B is that of the model trained on all the $C = 100$ classes. A downstream classifier always obtain the best performance over the latter.

embed the same sample subset (again, the samples for the selected M classes). We then train two downstream classifiers to classify the sample label from the embeddings: one over the embeddings obtained by the task-specific model and one over the embeddings produced by the model trained on the whole dataset. We pick $M = 30$ and $C = 100$ for CIFAR100. Intuitively, if the features learned by the task-specific model were better specialized, the classification accuracy of the downstream classifier would be higher than when trained over the features learned by the global model. We can see in fig. 14 that this is not the case, as in any of the four attempts the features of the global model (space B) result in a greater accuracy. As before, the restriction over the M classes in the space of a model trained on all C classes proves a better feature space than the space of a model that is only trained over the M classes, again disconfirming hypothesis A in section 4.3.

Appendix C. Background

C.1. Relative representations

Relative representations encode data points as distances with respect to a set of training points termed anchors. Moschella et al. (2023) empirically show that in many scenarios two spaces become aligned when passing to this distance-based representation, claiming that stochasticities in the training process often result in an angle-preserving transformation between the two latent spaces. Figure 15 shows a visual representation of the relative representation framework.

C.2. Similarity measures

The most common representational similarity measure is CKA (Kornblith et al., 2019), that is defined as:

$$m_{\text{CKA}}(\mathbf{R}, \mathbf{R}') = \frac{\text{HSIC}(\mathbf{S}, \mathbf{S}')}{\sqrt{\text{HSIC}(\mathbf{S}, \mathbf{S})\text{HSIC}(\mathbf{S}', \mathbf{S}')}}, \quad (3)$$

where $\text{HSIC}(\mathbf{S}, \mathbf{S}') = \frac{1}{(N-1)^2} \text{tr}(\mathbf{S}\mathbf{H}\mathbf{S}'\mathbf{H})$, $\mathbf{H} = \mathbf{I} - \frac{1}{N}\mathbf{1}\mathbf{1}^\top$ is a centering matrix, and $\mathbf{1}$ is a vector of N ones. The denominator is introduced to scale CKA between 0 and 1, with a value of 1 indicating equivalent representations. We employ the linear kernel version, as the difference with more complex kernels is usually negligible (Kornblith et al., 2019).

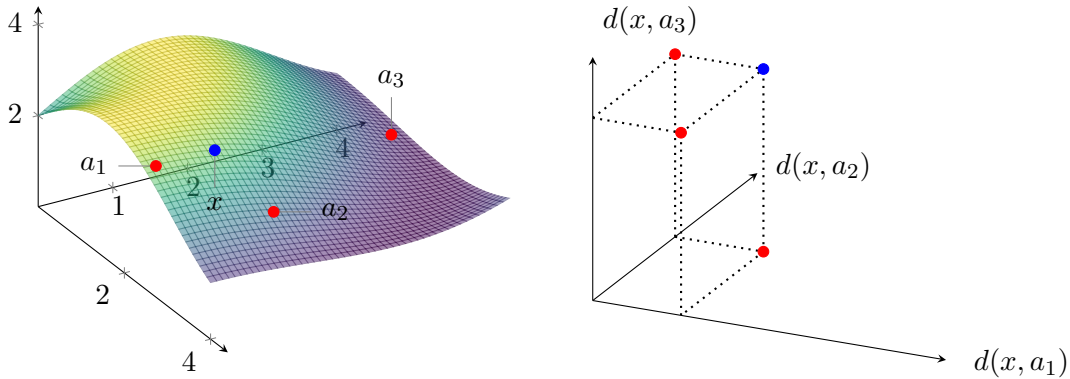


Figure 15: Relative representations: (left) a sample x and three anchor samples a_1, a_2, a_3 are embedded in a latent space. (right) the new representation of x is given by its distance with respect to the anchors.

Most notably, CKA is invariant to orthogonal transformations and isotropic scaling, assuming invariant similarity measures for RSM computation. It is worth remarking that relative representations are invariant to angle-preserving transformations, a superclass of the orthogonal transformations.

C.3. Separability measures

Let's denote the aggregated space as $\mathbf{X}_{\text{aggregated}}$. For simplicity, consider a scenario where the aggregated space consists of samples from two different classes C_1 and C_2 . The goal is to assess the separability of these two classes in the aggregated space. To do so, we first calculate the centroid (mean vector) for each class in the aggregated space:

$$\mathbf{c}_{C_1} = \frac{1}{|C_1|} \sum_{x \in C_1} \mathbf{x}$$

$$\mathbf{c}_{C_2} = \frac{1}{|C_2|} \sum_{x \in C_2} \mathbf{x}$$

Then, we calculate the Euclidean distance between the centroids of the two classes:

$$d_{\text{inter}} = \|\mathbf{c}_{C_1} - \mathbf{c}_{C_2}\|$$

as well as the average distance of samples in each class to their respective centroid:

$$d_{\text{intra}_{C_1}} = \frac{1}{|C_1|} \sum_{x \in C_1} \|\mathbf{x} - \mathbf{c}_{C_1}\|$$

$$d_{\text{intra}_{C_2}} = \frac{1}{|C_2|} \sum_{x \in C_2} \|\mathbf{x} - \mathbf{c}_{C_2}\|$$

A separability score can then be defined as the ratio of inter-class distance to the average intra-class distance:

$$S = \frac{d_{\text{inter}}}{\frac{1}{2}(d_{\text{intra}_{C_1}} + d_{\text{intra}_{C_2}})}$$

Intuitively, an high value of S indicates that the classes are well-separated in the aggregated space, meaning there is little to no collision, while a value that is close to or less than 1 indicates that there is a significant overlap or collision of classes in the aggregated space. For a set of classes, we generalize the above approach by calculating pairwise separability scores for all combinations of class pairs and then taking the average or the minimum of these scores as an overall indicator.